01 Nov 2023

Boosting SNR Of Cascaded FBGs In A Sapphire Fiber Through A Rapid Heat Treatment

Farhan Mumtaz
Missouri University of Science and Technology, mfmawan@mst.edu

Hanok Tekle

Bohong Zhang

Jeffrey D. Smith
Missouri University of Science and Technology, jsmith@mst.edu

et. al. For a complete list of authors, see https://scholarsmine.mst.edu/ele_comeng_facwork/5180

Recommended Citation

F. Mumtaz et al., "Boosting SNR Of Cascaded FBGs In A Sapphire Fiber Through A Rapid Heat Treatment," *Optics Letters*, vol. 48, no. 21, pp. 5703 - 5706, Optica Publishing Group, Nov 2023.
The definitive version is available at https://doi.org/10.1364/OL.506053

Letter

Vol. 48, No. 21 / 1 November 2023 / *Optics Letters* 5703

Optics Letters

Boosting SNR of cascaded FBGs in a sapphire fiber through a rapid heat treatment

Farhan Mumtaz,[1,3] **Hanok Tekle,**[2] **Bohong Zhang,**[1] **Jeffrey D. Smith,**[2] **Ronald J. O'Malley,**[2] **Rex E. Gerald II,**[1] **and Jie Huang**[1,*]

[1] *Department of Electrical and Computer Engineering, Missouri University of Science and Technology, Rolla, Missouri 65409-0040, USA*
[2] *Department of Material Science & Engineering, Missouri University of Science and Technology, Rolla, Missouri 65409-0040, USA*
[3] *mfmawan@mst.edu*
**jieh@mst.edu*

Received 15 September 2023; revised 9 October 2023; accepted 9 October 2023; posted 10 October 2023; published 24 October 2023

This Letter reports the performance of femtosecond (fs) laser-written distributed fiber Bragg gratings (FBGs) under high-temperature conditions up to 1600°C and explores the impact of rapid heat treatment on signal-to-noise ratio (SNR) enhancement. FBGs are essential for reliable optical sensing in extreme temperature environments. Comprehensive tests demonstrate the remarkable performance and resilience of FBGs at temperatures up to 1600°C, confirming their suitability for deployment in such conditions. The study also reveals significant fringe visibility improvements of up to ∼10 dB on a 1-m-long sapphire optical fiber through rapid heat treatment, representing a first-time achievement to the best of our knowledge. These enhancements are vital for improving the SNR and overall performance of optical fiber systems in extreme temperatures. Furthermore, the research attains long-term stability for the cascaded FBGs over a 24-hr period at 1600°C. This research expands our understanding of the FBG behavior in high-temperature environments and opens avenues for developing robust optical fiber systems for energy, aerospace, oil and gas, and high-temperature distributed sensing applications.

https://doi.org/10.1364/OL.506053

FBGs have emerged as crucial components in optical sensing systems, offering advantages such as high sensitivity, compact size, and immunity to electromagnetic interference [1]. They find applications in various industries, including aerospace, oil and gas, structural monitoring, and high-temperature sensing [2]. However, the performance and reliability of FBGs in extreme temperature environments remain a significant challenge. The effects of high temperatures on conventional FBGs include spectral distortion, signal attenuation, and reduced SNR [3]. To overcome these limitations, researchers have explored alternative materials and fabrication techniques to enhance the performance of FBGs in harsh temperature conditions. The fs-laser writing has emerged as a promising method for inscribing FBGs with high precision and control, enabling the fabrication of FBGs in various materials, including specialty fibers with superior thermal properties [4]. Sapphire fibers have attracted considerable attention due to their exceptional mechanical and thermal stability. They offer high-temperature resistance, chemical inertness, and low-loss characteristics, making them suitable for extreme temperature sensing applications [5,6]. Fs-laser-written FBGs in sapphire fibers have shown promising performance and potential for high-temperature sensing [7].

Several studies have demonstrated the advantages of fs-laser-written FBGs in various materials. For instance, He *et al.* [8] reported the fabrication of FBGs in photosensitive fibers using fs-laser pulses, achieving high reflectivity and thermal stability. Mihailov *et al.* [9] investigated the thermal stability and mechanical reliability of fs-laser-written FBGs in silica fibers, highlighting their robustness for high-temperature sensing applications. Furthermore, significant progress has been made in the fabrication and characterization of sapphire-fiber-based FBGs for high-temperature sensing applications. Busch *et al.* [10] examined the stability of sapphire FBGs under temperature cycles and annealing conditions. Over a period of 4 weeks, temperature cycles between 500°C and 1200°C showed no signs of wavelength or intensity drifts. Annealing at higher temperatures prevented a wavelength drift but did not lead to a significant improvement in the peak. However, at 1745°C, the peak intensity decreased to 60% of its initial value. Shi *et al.* [11] introduced a heat treatment technique for three cascaded FBGs inscribed via the point-by-point method on 60 cm sapphire fiber. The heat treatment resulted in a remarkable enhancement of up to 5 dB in the fringe visibility of the cascaded FBGs, improving their temperature sensing capabilities. In a similar vein, Yang *et al.* [12] reported the successful inscription of three cascaded point-by-point FBGs in a 95 cm sapphire fiber for commercial boiler application. After slowly annealing the fiber for 80 h at a temperature of 1000°C, they achieved a fringe visibility of 4.5 dB in the reflection spectrum, further emphasizing the potential of sapphire-fiber-based FBGs for high-temperature sensing applications. In a separate study [13], they reported a process of slow annealing sapphire FBG at a temperature of 1400°C for a duration of 6 h, which amplify the fringe visibility on a linear scale, increasing it from 200 a.u. to 1200 a.u. Habisreuther *et al.* [14] conducted research on the performance of a single FBG inscribed into a sapphire fiber of less than 1 m in length with a diameter of 100 µm. They subjected the FBG

to testing under an inductive furnace environment with a flow of Argon gas, reaching temperatures of up to 1900°C. The study achieved a temperature resolution of ±2 K, demonstrating the potential of sapphire-fiber-based FBGs for accurate and reliable high-temperature sensing applications. Guo *et al.* [15] conducted a study on the fabrication of line-by-line FBGs on a sapphire fiber with a diameter of 60 µm and a length of 20 cm. They successfully achieved a fringe visibility of 10 dB with a single FBG. The FBG was then subjected to testing under high-temperature conditions, reaching temperatures up to 1600°C. This research highlights the feasibility of using line-by-line FBGs on sapphire fibers for high-temperature sensing applications, showcasing their potential for enhanced performance in extreme temperature environments. Grobnic [16] conducted research on the fabrication of a single line-by-line written FBG on a sapphire fiber with a length of 25 cm and a diameter of 125 µm. The study achieved a fringe visibility of 6.5 dB for the FBG and successfully demonstrated temperature measurements up to 1500°C. Xu *et al.* [17] successfully demonstrated the fabrication of five line-by-line cascaded FBGs on a 60 µm diameter sapphire fiber, achieving 4 dB fringe visibility in the cascaded configuration. Furthermore, they compared the SNR between 60 µm and 100 µm diameter sapphire fibers, finding that the smaller diameter fiber exhibited superior SNR. These findings highlight the potential of line-by-line cascaded FBGs on smaller diameter sapphire fibers for improved sensing performance in high-temperature application. Recently, our research group successfully implemented large-scale cascading of sapphire FBGs using a first-order point-by-point FBG fabrication technique [18]. This achievement exemplifies the effective generation of well-distributed thermal mapping, particularly suitable for applications in harsh environments. Recent studies highlight the growing interests in sapphire-fiber-based FBGs and their potential for high-temperature sensing applications. By incorporating these advancements into our research, we aim to deepen our understanding of the performance and capabilities of fs-laser-written FBGs in sapphire highly multimode fiber under extreme temperature conditions.

In previous studies, stability was demonstrated at elevated temperatures, specifically reaching a maximum of 1200°C while achieving a fringe visibility of approximately 5 dB (~3.5 a.u. in linear intensity) [11,12]. These studies utilized a slow annealing technique to enhance the SNR of cascaded FBGs, resulting in an improvement of approximately 0.5 a.u. However, these FBGs tend to degrade in harsh environments. Slow annealing involves controlled heating and cooling cycles that induce structural changes, resulting in improved performance and stability at high temperatures. Nevertheless, the effects of rapid heat treatment annealing on fs-laser-written FBGs in a sapphire highly multimode fiber at extreme temperatures have not been investigated before. This study aims to examine long-term stability performance and the impact of rapid heat treatment as an alternative approach to enhancing the fringe visibility of cascaded FBGs in a 1-m-long sapphire highly multimode fiber. By comparing the performance of rapid heat treatment with the results obtained from slow annealing, we seek valuable insights into the optimal methods for enhancing FBG performance in high-temperature environments, specifically at temperatures up to 1600°C.

Figure 1(a) presents a schematic representation of the line-by-line method employed for the precise fabrication of three cascaded FBGs using fs-laser inscription. The process involved

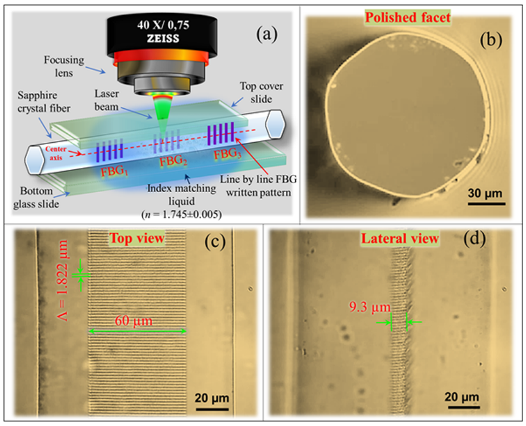

Fig. 1. (a) Schematic representation of the fs-laser inscription pattern employed for cascaded line-by-line fabrication of FBGs, while the micrographs exhibit (b) polished facet of a sapphire crystal fiber, and the line spacing patterns for FBG_3 displaying (c) top view and (d) lateral view.

a Spectra Physics Sp-One-8-SHG laser integrated with a second-harmonic generation module, allowing customization of the central wavelength range (520 nm or 1040 nm). Laser parameters were adjusted to generate 520 nm pulses at a repetition rate of 5 kHz with a target energy of 500 nJ. Accurate placement of the inscriptions was ensured by employing a 3D alignment assembly (Newport, XMS100) along with the fs laser. The laser pulse energy was regulated using a half-wave plate and a Glan laser polarizer. The pulses were directed through dichroic mirrors and focused onto the target object using a 40× non-immersion objective lens (ZEISS). Throughout the fabrication process, positioning and monitoring of the target object were facilitated by a CCD camera. The laser system was operated via a user-friendly graphical user interface (GUI)-based computer-aided device, providing comprehensive control over predefined operations. The phase matching condition of the FBGs is given by $m\lambda_B = 2n_{eff}\Lambda$ [19], where m represents the FBG order, λ_B is the wavelength, n_{eff} is the effective refractive index, and Λ is the grating period. A sapphire fiber with a diameter of 125 µm and a length of 1 m (purchased from Micromaterials Inc., USA) was utilized, having a refractive index of 1.745 at 1550 nm. An index-matching liquid (purchased from Cargille–Sachher Lab Inc. USA) with a refractive index of 1.745 ± 0.005 was employed between the glass cover slides during the fabrication process to facilitate the visualization of localized changes in the sapphire fiber induced by the femtosecond laser. Fourth-order cascaded FBGs were fabricated with $m = 4$, and the corresponding Λ values for FBG_1, FBG_2, and FBG_3 were 1.685 µm, 1.754 µm, and 1.822 µm, respectively. The cascaded FBGs lengths were set at 7 mm, 8 mm, and 9 mm, while maintaining a constant reflector width of 60 µm. The polished cross section of the sapphire crystal fiber (approximately 125 µm in diameter) is depicted in Fig. 1(b), while Figs. 1(c) and 1(d) illustrate top view and lateral view of the fs-laser-written reflector's width and depth for FBG_3. The FBGs were inscribed at intervals of 20 mm from each other, and FBG_3 was positioned near the end facet of the sapphire fiber.

Figure 2(a) illustrates the experimental setup employed to record the reflection interference spectrum. The sapphire optical fiber was spliced with a multimode fiber (MMF) using the glass processor splicing method described in our previous study

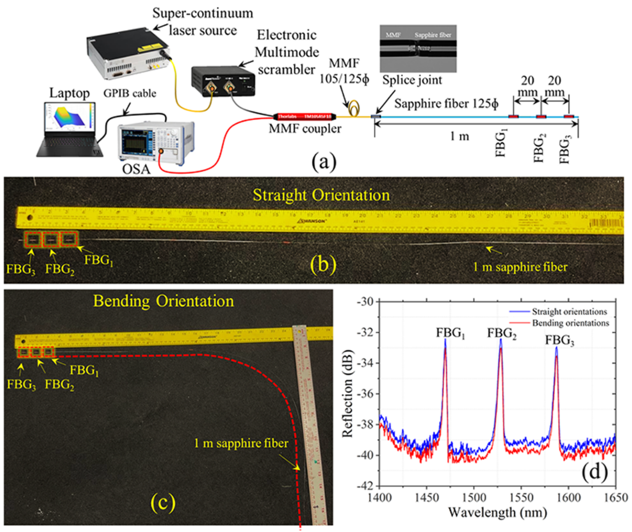

Fig. 2. (a) Schematic illustration of the signal acquisition setup for cascaded sapphire FBGs. (b) Visual representation depicting the sapphire fiber with cascaded FBGs in a straight orientation. (c) The same representation but with a bending orientation. (d) Interference spectra observed from cascaded sapphire FBGs in both straight and bending orientations.

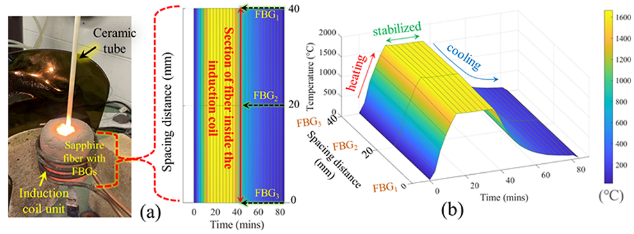

Fig. 3. (a) The 2D temperature distribution plot shows the placement of the FBGs inside the induction coil region. Additionally, a real experimental image of the induction coil unit is displayed when the temperature reaches 1600°C. (b) The 3D contour plot illustrates the transient profile of the temperature during the heating, stabilizing, and cooling phases.

[19]. To minimize the impact of multimodal interferences and improve the SNR, an electronic mode scrambler (MMS-201) was utilized. The input light for the FBG sensors was provided by a supercontinuum laser source (SC-5, Wuhan Yangtze Soton Laser). An optical spectrum analyzer (OSA) was employed to capture the changes in the spectrum. The OSA was connected to a laptop using a GPIB cable, and the experimental data was recorded using a custom MATLAB program code. The purpose of the setup was to investigate the effects of different orientations of the sapphire fiber, both straight and bent.

The sapphire fiber was subjected to both straight and bending orientations to assess variations in FBGs' signal strength, as depicted in Figs. 2(b) and 2(c). Notably, when the sapphire fiber underwent a bend of approximately 90° with a substantial curvature, the reflection signal displayed minimal attenuation, as evident in the interferogram showcased in Fig. 2(d). Sapphire fibers are highly multimode, and typically bending can significantly affect the signal strength. However, the findings of the experiment demonstrated that the signal remained stable without any significant dropout, representing a significant breakthrough. This breakthrough allows for the implementation of such configurations in scenarios necessitating bending applications.

Afterward, the cascaded sapphire FBGs were placed inside an induction coil furnace for a rapid heat treatment. The sapphire fiber was encased in a 24 in. nonporous Alumina Ceramic Tube, which had two bores. The outer diameter of the tube was 0.250 in., while the inner diameter measured 0.063 in. This ceramic tube provided a protective sheath for the fiber, ensuring its safety and stability during the experimental process. The induction coil system had a ramp rate of 100°C/min, allowing for rapid temperature increase. The temperature was raised until it reached 1600°C and then stabilized for approximately 30 min. Subsequently, the temperature was gradually ramped down. Moreover, a 2D profile depicting the temperature gradient was created, illustrating the positioning of the FBGs within the induction coil furnace and the respective time intervals for each segment, as shown in Fig. 3(a), which also includes a real experimental image of the induction coil unit for visual reference. To gain a clearer understanding of the different steps involved in the rapid heat treatment process, a 3D contour plot was created, as shown in Fig. 3(b). This plot depicted the heating, stabilizing, and cooling intervals, providing a visual representation of the temperature profile.

Observations reveal that the sapphire-fiber section within the induction furnace endured an extreme temperature environment, characterized by a temperature gradient spanning from 1550°C to 1600°C. Following the cooling process, a comparative analysis was conducted between the interferogram acquired from the cascaded FBGs post-heat treatment and the interferogram obtained before the heat treatment. Substantial improvements in the SNR were evident. Specifically, each FBG exhibited an average 3 dB gain, resulting in fringe enhancement within the interferogram, as illustrated in Fig. 4(a). Notably, a fringe visibility of 10 dB was achieved, underscoring the efficacy of the annealing process in significantly enhancing the SNR of the FBGs through a rapid heat treatment. Further discussion related to the rapid annealing of sapphire FBGs can be found in Supplement 1.

Following the rapid heat treatment, three cascaded FBGs with Bragg wavelengths of 1469.41 nm, 1528.12 nm, and 1587.07 nm underwent calibration. The calibration process involved employing a customized high-temperature furnace (SAFTherm SANTE FURNACE 30–1700°C) with a precision of ±1°C and a maximum temperature capability of 1700°C, as ascertained by a B-type thermocouple. The FBG was positioned within the furnace, which featured a controlled heating rate of 5°C per minute. During the calibration procedure, the temperature incrementally rose from an ambient room temperature at 1600°C, progressing in 100°C increments. Conversely, for the cooling phase, the FBG underwent a reverse process, with temperature data recorded in 100°C decrements. Throughout both the heating and cooling phases, the temperature remained constant for 30 min at each heating step, and the spectrum was captured using an OSA. The spectral evolution of cascaded FBGs during the heating process is illustrated in Fig. 4(b). Notably, each FBG exhibits an excellent fit to a 2nd-order polynomial curve. The curve fitting results in R-squared values of approximately 0.999 for both the temperature increase and decrease, as illustrated in Fig. 4(c).

The stability assessment of the cascaded FBGs was conducted at an elevated temperature of 1600°C. The sensor exhibited commendable stability performance throughout a rigorous 24-hr

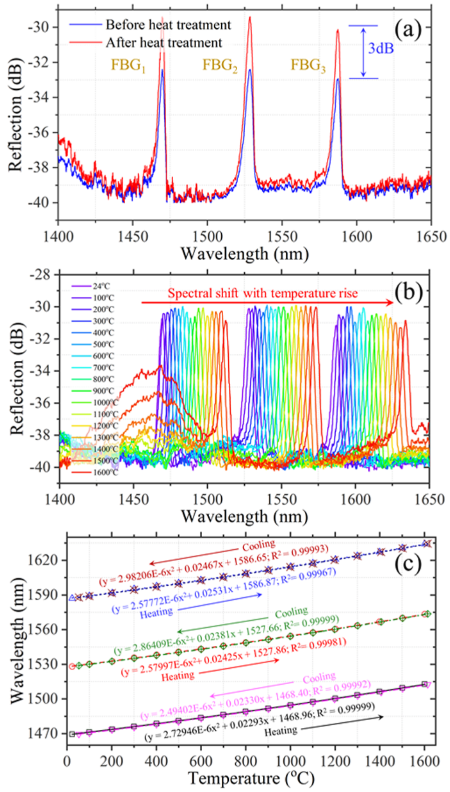

Fig. 4. (a) Interferogram before and after the rapid heat treatment. (b) Spectral evolution of the FBG sensors during the heat treatment process, spanning from 24°C to 1600°C. (c) Calibration curves of sapphire FBGs, showcasing their responses during heating and cooling phases.

duration in this challenging environmental condition. Detailed experimental demonstrations and precautionary measurement procedures for this test can be found in Supplement 1 and in Ref. [20].

In summary, this research demonstrated the excellent performance of cascaded line-by-line FBGs written on a 1-m-long sapphire fiber for distributed temperature mapping under harsh environmental conditions. The study establishes the long-term stability of these FBGs, sustaining good performance over a continuous 24-hr period at 1600°C. This achievement surpasses previous reports, which had demonstrated a stability of up to 1200°C using three cascaded FBGs [11] or up to 1600°C with a single FBG [21]. The highly multimode nature of sapphire fibers presents a considerable challenge in achieving enhanced fringe visibility. However, through the implementation of the rapid heat treatment, ∼3 dB improvements in SNR were achieved, surpassing previous achievements with slow annealing methods and shorter sapphire fibers. The obtained interferograms exhibited fringe visibility of ∼10 dB, a significant achievement considering the inherent multimode behavior of sapphire fibers. The successful annealing process achieved through the rapid heat treatment holds great potential for enhancing FBG performance in extreme temperature environments. These findings expand our understanding of the FBG behavior under high-temperature conditions and offer promising prospects for the development of robust optical fiber systems. The utilization of rapid heat treatment techniques could pave the way for improved performance in energy, aerospace, oil and gas, and high-temperature sensing applications. Further research and optimization in this arena hold promise for overcoming the challenges posed by the highly multimode nature of sapphire fibers and unlocking their full potential in harsh temperature sensing applications.

Funding. U.S. Department of Energy's Office of Energy Efficiency and Renewable Energy (DE-EE0009119).

Acknowledgment. This material is based upon the work supported by the US Department of Energy's Office of Energy Efficiency and Renewable Energy (EERE) under the Advanced Manufacturing Office (AMO) Award Number DE-EE0009119. The views expressed herein do not necessarily represent the views of the U.S. Department of Energy or the United States Government.

Disclosures. The authors declare no conflicts of interest.

Data availability. Access to the underlying data supporting the results reported in this article can be requested from the corresponding author in a reasonable manner.

Supplemental document. See Supplement 1 for supporting content.

REFERENCES

1. D. Kinet, P. Mégret, and K. W. Goossen, *et al.*, Sensors **14**, 7394 (2014).
2. C. Zhu, R. E. Gerald, and J. Huang, IEEE Trans. Instrum. Meas. **69**, 8639 (2020).
3. K. O. Hill, Y. Fujii, and D. C. Johnson, *et al.*, Appl. Phys. Lett. **32**, 647 (1978).
4. K. O. Hill and G. Meltz, J. Lightwave Technol. **15**, 1263 (1997).
5. F. Mumtaz, M. Aqueel Ashraf, and Y. Dai, *et al.*, Results Phys. **18**, 103311 (2020).
6. F. Mumtaz, Y. Dai, and M. A. Ashraf, *et al.*, Prog. Electromagn. Res. C **107**, 219 (2021).
7. B. Wang, Y. Niu, and X. Qin, *et al.*, Measurement **184**, 109868 (2021).
8. J. He, Y. Wang, and C. Liao, *et al.*, Sci. Rep. **6**, 23379 (2016).
9. S. J. Mihailov, D. Grobnic, and C. Hnatovsky, *et al.*, Sensors **17**, 2909 (2017).
10. M. Busch, W. Ecke, and I. Latka, *et al.*, Meas. Sci. Technol. **20**, 115301 (2009).
11. G. Shi, R. Shurtz, and G. Pickrell, *et al.*, Opt. Lett. **47**, 4724 (2022).
12. S. Yang, D. Homa, and H. Heyl, *et al.*, Proc. SPIE 11000, Fiber Optic Sensors and Applications XVI **11000** , 1100002 (2019), .
13. S. Yang, D. Hu, and A. Wang, Opt. Lett. **42**, 4219 (2017).
14. T. Habisreuther, T. Elsmann, and Z. Pan, *et al.*, Appl. Therm. Eng. **91**, 860 (2015).
15. Q. Guo, Y. Sen Yu, and Z. M. Zheng, *et al.*, IEEE Trans. Nanotechnol. **18**, 208 (2019).
16. D. Grobnic, S. J. Mihailov, and C. W. Smelser, *et al.*, IEEE Photonics Technol. Lett. **16**, 2505 (2004).
17. X. Xu, J. He, and C. Liao, *et al.*, Opt. Lett. **43**, 4562 (2018).
18. F. Mumtaz, T. Hanok, and B. Zhang, *et al.*, Opt. Lett. **48**, 4380 (2023).
19. F. Mumtaz, D. R. Alla, and M. Roman, *et al.*, Appl. Opt. **62**, 1392 (2023).
20. H. Chen, B. Michael, and R. O. Paul, *et al.*, Appl. Phys. Rev. **5**, 011102 (2018).
21. J. He, X. Xu, and B. Du, *et al.*, ACS Appl. Mater. Interfaces **14**, 12359 (2022).